

# Journal of Semiconductors

JOS

iopscience.iop.org/jos  
www.jos.ac.cn

## A $10 \times 10$ deep ultraviolet light-emitting micro-LED array

Huabin Yu, Muhammad Hunain Memon, Hongfeng Jia, Haochen Zhang, Meng Tian, Shi Fang, Danhao Wang, Yang Kang, Shudan Xiao, and Haiding Sun

Citation: H B Yu, M H Memon, H F Jia, H C Zhang, M Tian, S Fang, D H Wang, Y Kang, S D Xiao, and H D Sun, A  $10 \times 10$  deep ultraviolet light-emitting micro-LED array[J]. *J. Semicond.*, 2022, In Press .

View online: <http://www.jos.ac.cn/article/shaid/dd652d47634147103e01c5998ee426c06de68d2bbdc602d47c19010ab59af124>

## Articles you may be interested in

[The effect of AlN/AlGaIn superlattices on crystal and optical properties of AlGaIn epitaxial layers](#)

Journal of Semiconductors. 2017, 38(11), 113002 <https://doi.org/10.1088/1674-4926/38/11/113002>

[Preface to the Special Topic on Deep Ultraviolet Light-Emitting Materials and Devices](#)

Journal of Semiconductors. 2019, 40(12), 120101 <https://doi.org/10.1088/1674-4926/40/12/120101>

[Characteristics and techniques of GaN-based micro-LEDs for application in next-generation display](#)

Journal of Semiconductors. 2020, 41(4), 041606 <https://doi.org/10.1088/1674-4926/41/4/041606>

[Performance improvement of light-emitting diodes with double superlattices confinement layer](#)

Journal of Semiconductors. 2018, 39(11), 114005 <https://doi.org/10.1088/1674-4926/39/11/114005>

[Size effect on optical performance of blue light-emitting diodes](#)

Journal of Semiconductors. 2019, 40(10), 102301 <https://doi.org/10.1088/1674-4926/40/10/102301>

[Fabrication of flexible AlGaInP LED](#)

Journal of Semiconductors. 2020, 41(3), 032302 <https://doi.org/10.1088/1674-4926/41/3/032302>



关注微信公众号，获得更多资讯信息

# A 10 × 10 deep ultraviolet light-emitting micro-LED array

Huabin Yu, Muhammad Hunain Memon, Hongfeng Jia, Haochen Zhang, Meng Tian, Shi Fang, Danhao Wang, Yang Kang, Shudan Xiao, and Haiding Sun<sup>†</sup>

School of Microelectronics, University of Science and Technology of China, Hefei 230026, China

**Abstract:** In this work, we design and fabricate a deep ultraviolet (DUV) light-emitting array consisting of 10 × 10 micro-LEDs ( $\mu$ -LEDs) with each device having 20  $\mu\text{m}$  in diameter. Strikingly, the array demonstrates a significant enhancement of total light output power by nearly 52% at the injection current of 100 mA, in comparison to a conventional large LED chip whose emitting area is the same as the array. A much higher (~22%) peak external quantum efficiency, as well as a smaller efficiency droop for  $\mu$ -LED array, was also achieved. The numerical calculation reveals that the performance boost can be attributed to the higher light extraction efficiency at the edge of each  $\mu$ -LED. Additionally, the far-field pattern measurement shows that the  $\mu$ -LED array possesses a better forward directionality of emission. These findings shed light on the enhancement of the DUV LEDs performance and provide new insights in controlling the light behavior of the  $\mu$ -LEDs.

**Key words:** AlGaIn; deep ultraviolet; micro-LED array; light extraction efficiency

**Citation:** H B Yu, M H Memon, H F Jia, H C Zhang, M Tian, S Fang, D H Wang, Y Kang, S D Xiao, and H D Sun, A 10 × 10 deep ultraviolet light-emitting micro-LED array[J]. *J. Semicond.*, 2022, in press

## 1. Introduction

AlGaIn-based deep ultraviolet light-emitting diodes (LEDs) have been identified as the next-generation DUV light source owing to the narrow emission wavelength band, non-toxicity, lower power consumption, and compact size with a long lifetime<sup>[1, 2]</sup>. Up to now, they have attracted significant research interest owing to potential applications, including non-light-of-sight optical communication, sensing systems, sterilization, and medical phototherapy<sup>[3]</sup>. However, the implementation of DUV LEDs in those industrial applications is restrained from their limited wall-plug efficiency (WPE), poor external quantum efficiency (EQE), and low light output power (LOP)<sup>[4]</sup>. One of the main limiting factors of the poor optical performance for the DUV LED is the extremely low light extraction efficiency (LEE), which is less than 10%<sup>[2]</sup>. Such low LEE is mainly owing to three reasons. Firstly, a large number of the upward-traveling DUV photons can be absorbed by the p-type GaIn-based hole-injection layer or can be blocked by the p-contact metals<sup>[5]</sup>. Secondly, most of the downward-traveling DUV photons are constantly reflected due to the excessive difference in the refractive index by the multiple nitride epilayers, AlGaIn/sapphire, and sapphire/air interfaces<sup>[6]</sup>. Thirdly, unlike the visible LEDs, the DUV LEDs are based on the AlGaIn materials with high aluminum content, leading to the increased transverse magnetic/transverse electric (TM/TE) polarization ratio<sup>[7]</sup>. Since the propagation direction is perpendicular to the *c*-axis, the in-plane TM photons are extremely hard to be extracted to the external space<sup>[8]</sup>.

To enlarge the LEEs, many efforts have been continuously devoted to extracting more UV photons in the DUV LED chips. For extracting those upward-traveling DUV

photons, many strategies such as high-reflectivity metal contacts<sup>[9, 10]</sup>, meshed p-GaIn structure<sup>[11, 12]</sup>, and photonic crystal structure<sup>[13]</sup> have been reported. Moreover, a variety of micro/nanostructures, including the nano-lens<sup>[6, 14, 15]</sup>, a patterned sapphire substrate<sup>[16, 17, 18, 19]</sup> and localized surface plasmons<sup>[20]</sup>, have been demonstrated for reducing the total internal reflection (TIR)<sup>[21]</sup>, which can help to extract the downward-traveling DUV photons in the DUV LEDs. Besides, the optimization of the angle<sup>[22]</sup>, the geometric shape<sup>[23]</sup>, and the reflector of the sidewall<sup>[24, 25]</sup> has also been investigated to enhance the emission of the TM-polarized light arriving at the chip sidewalls.

Apart from these important investigations, the emerging DUV micro-LED ( $\mu$ -LED) device architecture and the preliminary device characterizations show its potential to enhance the EQE<sup>[26]</sup>, which could be attributed to the reduction of the re-absorption of sideways-traveling photons as revealed by a recent cathodoluminescence study<sup>[27]</sup>. However, it should be noted that each  $\mu$ -LED inevitably possesses very low LOP due to the reduced emission area, which seriously hindered their further applications. Therefore, it is necessary to build interconnected DUV  $\mu$ -LEDs to obtain large output power, called  $\mu$ -LED arrays. Recently, Floyd *et al.* found that DUV  $\mu$ -LED array structure can significantly reduce the thermal impedance of each  $\mu$ -LED and thus enhance the sidewall out-radiation of the self-generated heat<sup>[28]</sup>. However, so far, the underlying mechanism of performance enhancement for those  $\mu$ -LED arrays is still lacking, and no systematic investigation, particularly from an optical perspective, on the light propagation within each  $\mu$ -LED and its array has been carried out.

In this letter, we present a systematic study on the electrical and optical behavior of light-emitting arrays. We designed and fabricated two kinds of arrays. One array is composed of 10 × 10  $\mu$ -LEDs, with each device having 20  $\mu\text{m}$  in diameter, named as  $\mu$ -LED array (20  $\mu\text{m}$ ) and another array is made of 4 × 4  $\mu$ -LEDs with each device showing 50  $\mu\text{m}$  in diameter,

Correspondence to: H D Sun, [haiding@ustc.edu.cn](mailto:haiding@ustc.edu.cn)

Received 29 NOVEMBER 2021; Revised 23 DECEMBER 2021.

©2022 Chinese Institute of Electronics

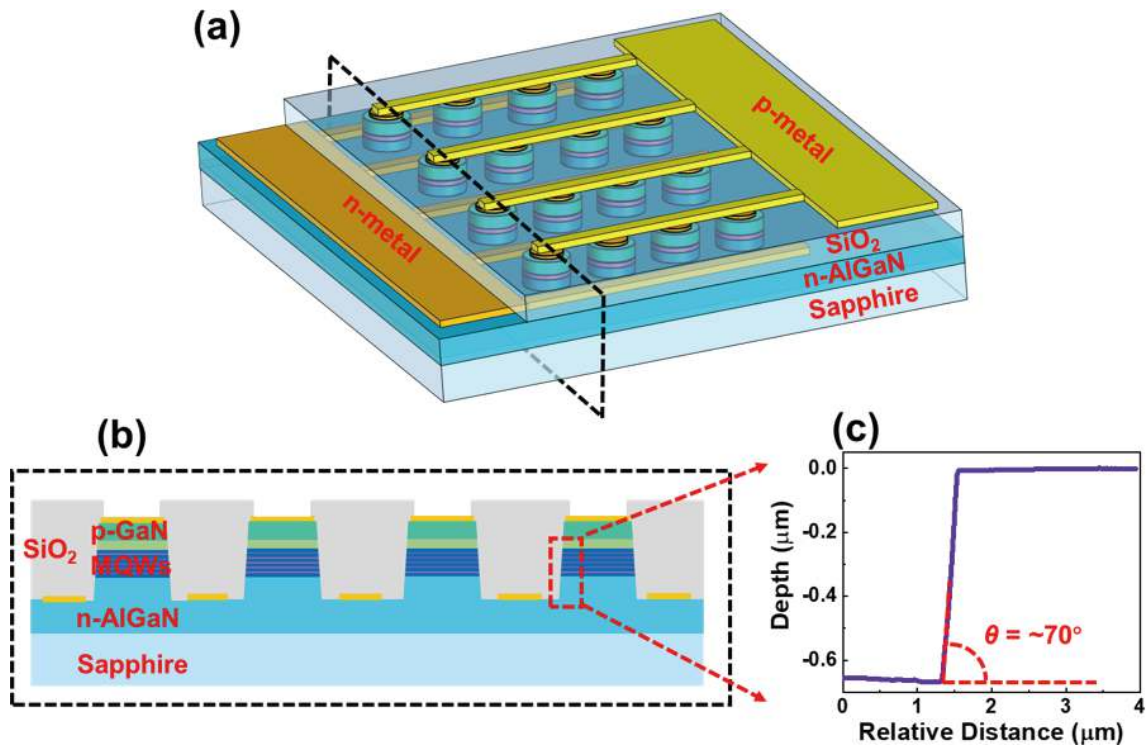


Fig. 1. (Color online) (a) Schematic of a fabricated DUV  $\mu$ -LED array and (b) its cross-section of the DUV  $\mu$ -LED array and (c) the profile of the sidewall and  $\theta$  is the inclination angle of the sidewall.

named as  $\mu$ -LED array ( $50\ \mu\text{m}$ ). At the same time, we fabricated a regular conventional LED (C-LED) whose surface-emitting area is identical to those two types of arrays. During the device test, we found that the  $\mu$ -LED array shows significantly boosted EQE, WPE, and LOP performance, owing to the enlarged LEE in each  $\mu$ -LED with a smaller chip size. The numerical finite-difference time-domain (FDTD) calculations have been implemented to better understand the light propagation behavior within LED chips with different chip sizes and to reveal the underlying mechanism of the LEE enhancement in  $\mu$ -LEDs.

## 2. Experiments

Similar to our previous report<sup>[26]</sup>, the epi-structure for our DUV LEDs consist of a  $2\text{-}\mu\text{m}$ -thick AlN buffer layer on the c-plane sapphire substrate, a  $2\text{-}\mu\text{m}$ -thick n-doped  $\text{Al}_{0.6}\text{Ga}_{0.4}\text{N}$  layer, a  $0.6\text{-}\mu\text{m}$ -thick n-doped  $\text{Al}_{0.48}\text{Ga}_{0.52}\text{N}$  layer followed by five periods  $\text{Al}_{0.45}\text{Ga}_{0.55}\text{N}/\text{Al}_{0.60}\text{Ga}_{0.40}\text{N}$  ( $2.5\ \text{nm}/10\ \text{nm}$ ) MQWs, a  $50\text{-nm}$ -thick p-doped  $\text{Al}_{0.70}\text{Ga}_{0.30}\text{N}$  electron blocking layer, and a  $350\text{-nm}$ -thick p-GaN. The wafers were fabricated into the truncated cone-shaped active mesas using the inductively coupled plasma (ICP) etching equipment. The C-LED has an emission area of  $200\ \mu\text{m}$  in diameter. The  $4 \times 4$  and  $10 \times 10\ \mu\text{-LED}$  arrays have chip size of  $50\ \mu\text{m}$  in diameter and  $20\ \mu\text{m}$  in diameter, respectively. We intended to keep the same total emission area for these three kinds of devices for performance comparison. Then, the metal stack of Ti/Al/Ni/Au ( $20/80/40/100\ \text{nm}$ ) as n-electrode and the Ni/Au ( $20/50\ \text{nm}$ ) as p-type contact was deposited by the electron beam evaporator. An  $800\text{-nm}$ -thick  $\text{SiO}_2$  film was deposited as an electrical insulation layer by using plasma-enhanced chemical vapor deposition (PECVD). Next, the  $\text{SiO}_2$  film on the n- and p-electrode was etched by the reactive ion etching (RIE) first and

then by the buffer oxide etchant (BOE). Finally, the Ni/Al/Ni/Au ( $20/500/100/120\ \text{nm}$ ) metal contacts were formed by the electron beam evaporator. The schematic of the  $\mu$ -LED array and its cross-section epi-structure are shown in Figs. 1(a) and 1(b), respectively.

The inclination angle of the sidewalls is around  $70^\circ$  which is characterized by the atomic force microscopy (AFM), as shown in Fig. 1(c). The electroluminescence (EL) spectra, the light output power, and the far-field emission for all the fabricated devices were measured from the back of the sapphire (not the epi-side) at room temperature. The far-field emission distribution of the LEDs was recorded by measuring the radiant intensity in angular steps of  $10^\circ$  on a three-axes rotation stage using a power meter at a distance of  $50\ \text{mm}$  from the LED chips.

## 3. Results and discussions

The current–voltage ( $I$ - $V$ ) curves for all the three investigated DUV LEDs are illustrated in Fig. 2(a). The forward voltages for the  $\mu$ -LED array ( $50\ \mu\text{m}$ ) and the  $\mu$ -LED array ( $20\ \mu\text{m}$ ) are slightly lower than that for the C-LED, as a result of the lower series resistance in the parallel device configuration and different n- contact areas. The inset of Fig. 2(a) shows the logarithmic plot of the forward  $I$ - $V$  curves. The reverse bias leakage values were as low as  $\sim 0.1\ \text{pA}$  at an applied voltage of  $-4\ \text{V}$ , showing the high quality of the as-grown epi-films and the low damage of the device during the dry-etching process. Notably, the  $\mu$ -LED array has a minor increase of leakage current than that of the C-LED, which could be attributed to the sidewall defects that may act as the current leakage pathways<sup>[29]</sup>. The EL spectra for the three devices at the injection current of  $100\ \text{mA}$  are shown in Fig. 2(b). The peak wavelength for all the devices is  $\sim 275\ \text{nm}$ ,

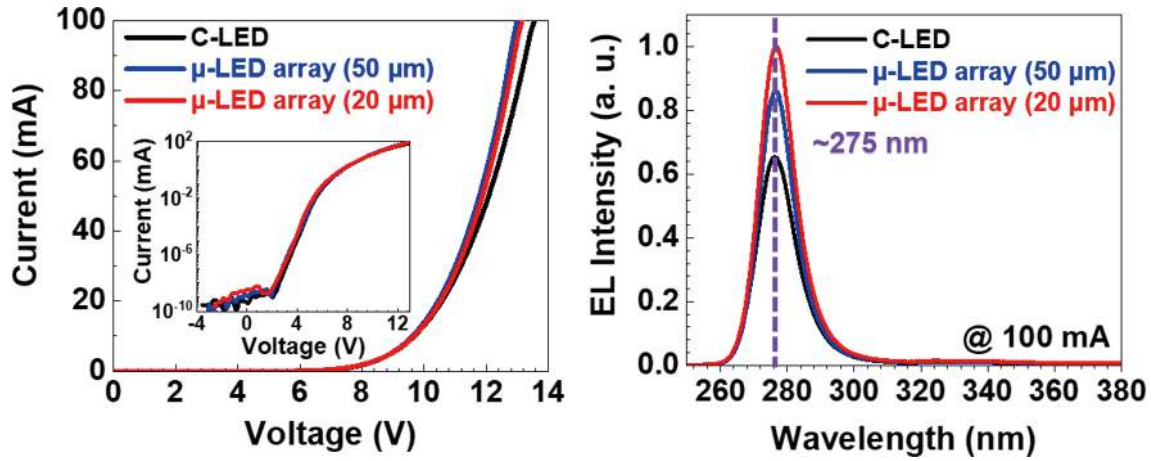


Fig. 2. (Color online) (a) The current–voltage ( $I$ – $V$ ) characteristic of the DUV LEDs. The inset shows the corresponding logarithmic plot. (b) The spectra of the DUV LEDs operating at the driving current of 100 mA.

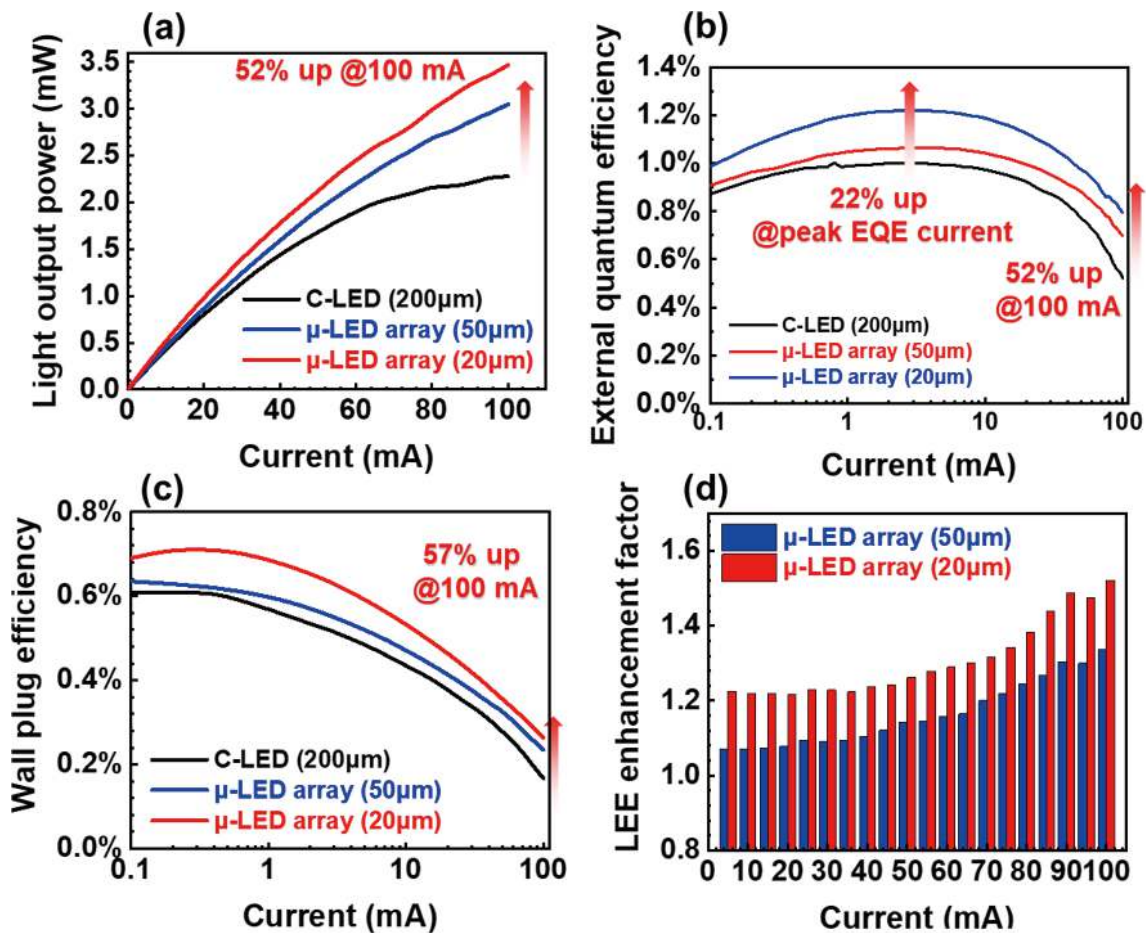


Fig. 3. (Color online) (a) The light output power (LOP), (b) the external quantum efficiency (EQE), (c) the wall-plug efficiency, and (d) the LEE enhancement factor of the DUV LEDs at different currents for the three investigated devices.

indicating that the change of the cone mesa size does not affect the emission wavelength. The EL emission intensity for the array is higher than that of the C-LED, and the  $\mu$ -LED with a smaller diameter shows a higher EL intensity, which provides an initial confirmation of the performance enhancement of the  $\mu$ -LED array.

As shown in Fig. 3(a), the  $\mu$ -LED array (50  $\mu\text{m}$ ) and the  $\mu$ -LED array (20  $\mu\text{m}$ ) exhibit a higher LOP by 34% and 52% than that of the C-LED under the injected current level of 100 mA, respectively. Notably, the LOP of the device gradually in-

creases with the increased injection current, but the LOP of C-LED reaches the maximum value at about 100 mA (the injected current density of 318 A/cm<sup>2</sup>) owing to the current injection saturation. Importantly, the  $\mu$ -LED array can sustain a much higher current injection. In the  $\mu$ -LED array, since the  $\mu$ -LEDs are interconnected in parallel, each  $\mu$ -LED is only injected several milliamperes under the total injection current of 100 mA, which is far from the current saturation. Therefore, the enhanced LOP leads to a significant higher EQE by 34% for the  $\mu$ -LED array (50  $\mu\text{m}$ ) and by 52% for the  $\mu$ -LED array

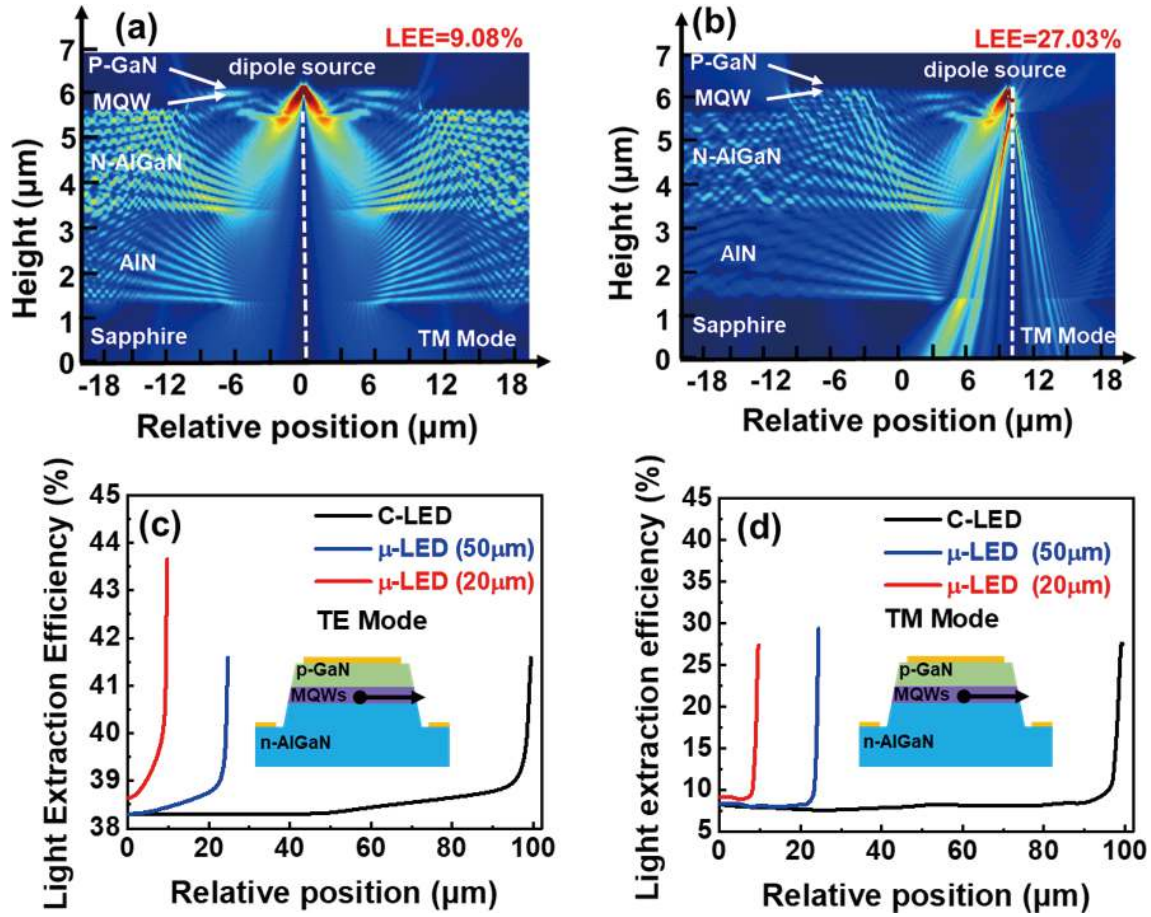


Fig. 4. (Color online) Electric field distributions for the light propagation paths of the TM-polarized light when the dipole source at (a) the center of the mesa and (b) the edge of the mesa. The LEEs for the (c) TE- and (d) TM-polarized light as a function of the position of the dipole source for the C-LED,  $\mu$ -LED (50  $\mu\text{m}$ ), and  $\mu$ -LED (20  $\mu\text{m}$ ), respectively. The insets of the (c) and (d) are the device schematic which indicates the position change of the dipole source.

(20  $\mu\text{m}$ ) at 100 mA, as displayed in Fig. 3(b). The peak EQE is 7% and 22% higher in the  $\mu$ -LED array (50  $\mu\text{m}$ ) and  $\mu$ -LED array (20  $\mu\text{m}$ ), respectively, in comparison to that of the C-LED. We also quantify the EQE droop levels at the injection current of 100 mA (the droop is defined as from highest to the lowest), which are 47.2%, 34.6%, and 34.1% for the C-LED, the  $\mu$ -LED array (50  $\mu\text{m}$ ), and the  $\mu$ -LED array (20  $\mu\text{m}$ ), respectively. Then, the WPE values of the LEDs can be calculated from LOP measurements by<sup>[2]</sup>,

$$\text{WPE} = \text{EQE} \cdot \text{CIE} = \text{LOP}/(IV) \quad (1)$$

From the calculation results shown in Fig. 3(c), the  $\mu$ -LED array (50  $\mu\text{m}$ ) has higher WPE by 40%, and  $\mu$ -LED array (20  $\mu\text{m}$ ) has higher WPE by 57% at 100 mA than that of the C-LED. This improvement is slightly larger than the EQE enhancement at 100 mA (34% for  $\mu$ -LED array (50  $\mu\text{m}$ ) and 52% for  $\mu$ -LED array (20  $\mu\text{m}$ )), due to the possible higher current injection efficiency (CIE) in the  $\mu$ -LED array configuration. Nevertheless, it can be explained that the enhancement of the WPE mainly lies in the effective improvement of EQE since all three LEDs have the same internal quantum efficiency (IQE) as they are fabricated on the same wafer. Therefore, there are ample reasons to explain that the enhancement of the LOP, EQE, and WPE is mainly attributed to the improvement of LEE. Furthermore, Fig. 3(d) shows the LEE enhancement factor<sup>[30]</sup> obtained by the ratio of EQE of the  $\mu$ -LED array to C-

LED. The LEEs of the  $\mu$ -LED array (50  $\mu\text{m}$ ) and  $\mu$ -LED array (20  $\mu\text{m}$ ) are approximately 1.3 times and 1.5 times higher in comparison with that of the C-LED, respectively. Moreover, the LEE enhancement factor of  $\mu$ -LED array is greater at higher injected current levels. These results indicate that the  $\mu$ -LED array can efficiently improve the LEE of the DUV LEDs.

To further reveal the underlying mechanism of the optical performance enhancement for the DUV  $\mu$ -LED array, we further use FDTD simulation to analyze the LEEs for C-LED and the  $\mu$ -LED arrays. In the simulation, a single dipole that served as the radiation source for the LED is located in the middle of the MQW layer<sup>[31]</sup>. Moreover, the perfectly matched layers (PMLs) are set around the LED, which can completely absorb the light escape from the simulation region. A power monitor is placed at 500 nm away from the bottom of the AlN layer to collect the photons that escape from the DUV LED. It is worth noting that we only set a single dipole in the MQW layer as the radiation source. Considering the possible co-existence of TM- and TE-polarized light, both LEEs of the TM- and the TE- polarized light with different mesa sizes are calculated. We also performed the LEE calculation by changing the position of the dipole source within the device.

As an example, the electric field distributions for the DUV  $\mu$ -LED (20  $\mu\text{m}$ ) are shown in Figs. 4(a) and 4(b). It can be observed that more DUV photons have been reflected on the sapphire side as the dipole source moves to the edge of the in-

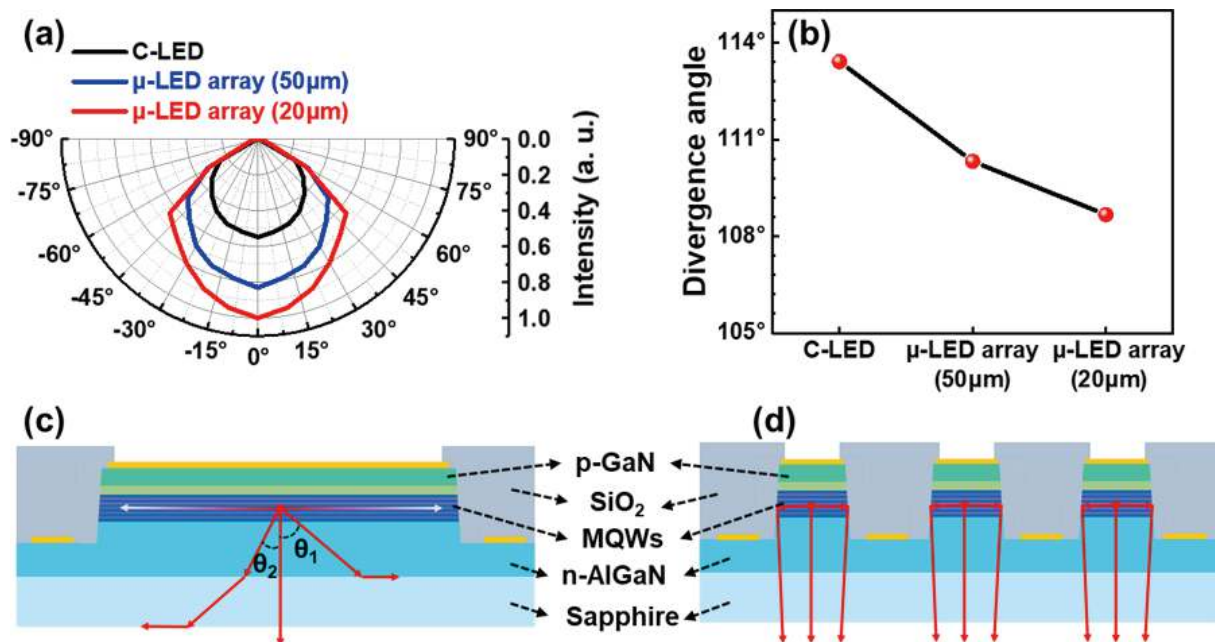


Fig. 5. (Color online) (a) Far-field patterns for the C-LED, the  $\mu$ -LED array (50  $\mu\text{m}$ ), and the  $\mu$ -LED array (20  $\mu\text{m}$ ) at 100 mA. (b) The divergence angle of the far-field patterns. The schematic illustrations of light propagation characteristics in (c) the C-LED and (d) the  $\mu$ -LED array.

clined sidewall. Furthermore, as shown in Figs. 4(c) and 4(d), it can be found that the LEEs of TM- and TE-polarized light increase as the dipole source moves to the mesa edge. Hence, we may conclude that the enhanced LEE of the  $\mu$ -LED is mainly benefitting from an enlarged ration of the sidewall area to the emission area. The smaller the device is, the larger the ratio becomes, which promotes higher LEE eventually.

Additionally, we also recorded the far-field radiation pattern of the C-LED, the  $\mu$ -LED array (50  $\mu\text{m}$ ), and the  $\mu$ -LED array (20  $\mu\text{m}$ ) at the injection current of 100 mA, which are presented in Fig. 5(a). A significantly stronger extracted light intensity was observed for the array over the entire angular radiation range compared with that of the C-LED. The  $\mu$ -LED array (20  $\mu\text{m}$ ) shows the highest light intensity. The spatial light intensities of all three samples reached to the maximum values at the emission angle of 0° when the devices were working at 100 mA. In Fig. 5(b), the divergence angle of the far-field patterns, extracted from Fig. 5(a), are 113.4°, 110.3°, and 108.7°, for the C-LED, the  $\mu$ -LED array (50  $\mu\text{m}$ ), and the  $\mu$ -LED array (20  $\mu\text{m}$ ), respectively. To better explain the phenomenon, schematic illustrations of light propagation characteristic in the C-LED and the  $\mu$ -LED array are exhibited in Figs. 5(c) and 5(d). In the C-LED, the severe TIR would block the downward-traveling DUV photons inside the device; meanwhile, the lateral-traveling DUV photons would be re-absorbed within a travel distance of  $\sim 15 \mu\text{m}$ <sup>[27]</sup>. In contrast, the  $\mu$ -LED array not only can shorten the lateral propagation distance of photons, thus reducing the chance to be re-absorbed but also can increase the chance to be reflected downwards by the inclined sidewall. Therefore, the  $\mu$ -LED array exhibits a higher light intensity with a smaller divergence angle (light propagation is more forward directionality).

#### 4. Conclusion

In summary, we have performed a systematic investiga-

tion on the electrical and optical performance of the DUV  $\mu$ -LED array. Compared with the C-LED, the DUV  $\mu$ -LED array (20  $\mu\text{m}$ ) shows a larger LOP by 52% at 100 mA with a higher peak EQE by 22% and a narrower divergence angle. Moreover, through the numerical analysis, it has been verified that the enlarged LEE for the  $\mu$ -LED array is attributed to an enhanced light reflection at the sidewall along with the shortened lateral propagation distance of photons. Hence, the DUV  $\mu$ -LED array with a smaller pixel size should exhibit better optical performance owing to the higher LEE. With an even smaller size (for example, 10  $\mu\text{m}$ ), a much higher LEE could be expected. Also, the light propagates with better directionality in the  $\mu$ -LED array. These observations offer a comprehensive understanding of the optical behavior in the  $\mu$ -LED array, which can help the community to build high-efficiency and high-power DUV LEDs for various applications.

#### Acknowledgements

This work was funded by the National Natural Science Foundation of China (Grant No. 52161145404, 61905236, 51961145110), the Fundamental Research Funds for the Central Universities (Grant No. WK2100230020), USTC Research Funds of the Double First-Class Initiative (Grant No. YD3480002002), and was partially carried out at the USTC Center for Micro and Nanoscale Research and Fabrication.

#### References

- [1] Zhang H C, Huang C, Song K, et al. Compositionally graded III-nitride alloys: Building blocks for efficient ultraviolet optoelectronics and power electronics. *Rep Prog Phys*, 2021, 84, 044401
- [2] Kneissl M, Seong T Y, Han J, et al. The emergence and prospects of deep-ultraviolet light-emitting diode technologies. *Nat Photonics*, 2019, 13, 233
- [3] Inagaki H, Saito A, Sugiyama H, et al. Rapid inactivation of SARS-CoV-2 with deep-UV LED irradiation. *Emerg Microbes Infect*, 2020, 9, 1744

- [4] Ren Z J, Yu H B, Liu Z L, et al. Band engineering of III-nitride-based deep-ultraviolet light-emitting diodes: A review. *J Phys D*, 2020, 53, 073002
- [5] Guttmann M, Susilo A, Sulmoni L, et al. Light extraction efficiency and internal quantum efficiency of fully UVC-transparent AlGaIn based LEDs. *J Phys D*, 2021, 54, 335101
- [6] Zheng Z H, Chen Q, Dai J N, et al. Enhanced light extraction efficiency via double nano-pattern arrays for high-efficiency deep UV LEDs. *Opt Laser Technol*, 2021, 143, 107360
- [7] Zhang J, Zhao H P, Tansu N. Effect of crystal-field split-off hole and heavy-hole bands crossover on gain characteristics of high Al-content AlGaIn quantum well lasers. *Appl Phys Lett*, 2010, 97, 111105
- [8] Floyd R, Hussain K, Mamun A, et al. Photonics integrated circuits using  $\text{Al}_x\text{Ga}_{1-x}\text{N}$  based UVC light-emitting diodes, photodetectors and waveguides. *Appl Phys Express*, 2020, 13, 022003
- [9] Peng X C, Guo W, Xu H Q, et al. Significantly boosted external quantum efficiency of AlGaIn-based DUV-LED utilizing thermal annealed Ni/Al reflective electrodes. *Appl Phys Express*, 2021, 14, 072005
- [10] Zhou S, Liu X, Gao Y, et al. Numerical and experimental investigation of GaN-based flip-chip light-emitting diodes with highly reflective Ag/TiW and ITO/DBR Ohmic contacts. *Opt Express*, 2017, 25, 26615
- [11] Zheng Y, Zhang Y, Zhang J, et al. Effects of meshed p-type contact structure on the light extraction effect for deep ultraviolet flip-chip light-emitting diodes. *Nanoscale Res Lett*, 2019, 14, 149
- [12] Zhang G, Shao H, Zhang M Y, et al. Enhancing the light extraction efficiency for AlGaIn-based DUV LEDs with a laterally over-etched p-GaN layer at the top of truncated cones. *Opt Express*, 2021, 29, 30532
- [13] Shin W, Pandey A, Liu X, et al. Photonic crystal tunnel junction deep ultraviolet light emitting diodes with enhanced light extraction efficiency. *Opt Express*, 2019, 27, 38413
- [14] Liang R L, Dai J N, Xu L L, et al. High light extraction efficiency of deep ultraviolet LEDs enhanced using nanolens arrays. *IEEE Trans Electron Devices*, 2018, 65, 2498
- [15] Inoue S I, Naoki T, Kinoshita T, et al. Light extraction enhancement of 265 nm deep-ultraviolet light-emitting diodes with over 90 mW output power via an AlN hybrid nanostructure. *Appl Phys Lett*, 2015, 106, 131104
- [16] Ooi Y K, Zhang J. Light extraction efficiency analysis of flip-chip ultraviolet light-emitting diodes with patterned sapphire substrate. *IEEE Photonics J*, 2018, 10, 1
- [17] Manley P, Walde S, Hagedorn S, et al. Nanopatterned sapphire substrates in deep-UV LEDs: Is there an optical benefit. *Opt Express*, 2020, 28, 3619
- [18] Yu H, Jia H, Liu Z, et al. Development of highly efficient ultraviolet LEDs on hybrid patterned sapphire substrates. *Opt Lett*, 2021, 46, 5356
- [19] Hu H P, Tang B, Wan H, et al. Boosted ultraviolet electroluminescence of InGaIn/AlGaIn quantum structures grown on high-index contrast patterned sapphire with silica array. *Nano Energy*, 2020, 69, 104427
- [20] Zhang C, Tang N, Shang L L, et al. Local surface plasmon enhanced polarization and internal quantum efficiency of deep ultraviolet emissions from AlGaIn-based quantum wells. *Sci Rep*, 2017, 7, 2358
- [21] Zhou S J, Xu H H, Tang B, et al. High-power and reliable GaIn-based vertical light-emitting diodes on 4-inch silicon substrate. *Opt Express*, 2019, 27, A1506
- [22] Chen Q, Zhang H X, Dai J N, et al. Enhanced the optical power of AlGaIn-based deep ultraviolet light-emitting diode by optimizing mesa sidewall angle. *IEEE Photonics J*, 2018, 10, 1
- [23] Lee J W, Park J H, Kim D Y, et al. Arrays of truncated cone AlGaIn deep-ultraviolet light-emitting diodes facilitating efficient out-coupling of in-plane emission. *ACS Photonics*, 2016, 3, 2030
- [24] Zhang J, Chang L, Zheng Y, et al. Integrating remote reflector and air cavity into inclined sidewalls to enhance the light extraction efficiency for AlGaIn-based DUV LEDs. *Opt Express*, 2020, 28, 17035
- [25] Tian M, Yu H, Memon M H, et al. Enhanced light extraction of the deep-ultraviolet micro-LED via rational design of chip sidewall. *Opt Lett*, 2021, 46, 4809
- [26] Yu H, Memon M H, Wang D, et al. AlGaIn-based deep ultraviolet micro-LED emitting at 275 nm. *Opt Lett*, 2021, 46, 3271
- [27] Floyd R, Gaevski M, Hussain K, et al. Enhanced light extraction efficiency of micropixel geometry AlGaIn DUV light-emitting diodes. *Appl Phys Express*, 2021, 14, 084002
- [28] Floyd R, Gaevski M, Alam M D, et al. An opto-thermal study of high brightness 280 nm emission AlGaIn micropixel light-emitting diode arrays. *Appl Phys Express*, 2021, 14, 014002
- [29] Ley R T, Smith J M, Wong M S, et al. Revealing the importance of light extraction efficiency in InGaIn/GaN microLEDs via chemical treatment and dielectric passivation. *Appl Phys Lett*, 2020, 116, 251104
- [30] Zhang S, Liu Y, Zhang J, et al. Optical polarization characteristics and light extraction behavior of deep-ultraviolet LED flip-chip with full-spatial omnidirectional reflector system. *Opt Express*, 2019, 27, A1601
- [31] Wei T B, Wu K, Lan D, et al. Selectively grown photonic crystal structures for high efficiency InGaIn emitting diodes using nano-spherical-lens lithography. *Appl Phys Lett*, 2012, 101, 211111



**Huabin Yu** received the BEng degree from University of Science and Technology of Beijing, Beijing, China, in 2019. He is pursuing the PhD-degree with the School of Microelectronics, University of Science and Technology of China, Hefei, China.



**Haiding Sun** received the BS degree from Huazhong University of Science and Technology, Wuhan, China, in 2008, and the PhD degree in electrical engineering from Boston University, Boston, MA, United States, in 2015. He is currently a professor with the School of Microelectronics, University of Science and Technology of China, Hefei, China. His research interests include the investigation of the physics, MBE and MOCVD epitaxy, fabrication, and characterization of semiconductor materials and devices.